Available online at www.sciencedirect.com
SCIENCE DIRECT®

Journal of the European Ceramic Society 24 (2004) 3261–3269

www.elsevier.com/locate/jeurceramsoc

Effect of matrix modification on tensile mechanical behavior of Tyranno® Si-Ti-C-O fiber-reinforced SiC matrix minicomposite at room and elevated temperatures

Shuqi Guo, Yutaka Kagawa*

Institute of Industrial Science, The University of Tokyo, 4-6-1, Komaba, Meguro-ku, Tokyo 153-8505, Japan

Received 25 July 2003; received in revised form 17 October 2003; accepted 25 October 2003

Abstract

The effect of the addition of borosilicate glass powder in the matrix on tensile mechanical behavior in an unidirectional Si-Ti-C-O fiber-reinforced SiC matrix minicomposite fabricated by the polymer infiltration pyrolysis (PIP) process has been studied. Tensile test of the minicomposite is carried out in an argon atmosphere at 298, 1273 and 1573 K. The Si-Ti-C-O/SiC shows a nearly linear tensile load–displacement curve which is similar to a dry fiber bundle independent of test temperature; conversely, the glass-powder-containing Si-Ti-C-O/SiC(g) exhibits a pronounced tensile load–displacement curve with a large nonlinear domain of deformation; however, this nonlinear domain became smaller at 1573 K. The matrix cracking load of Si-Ti-C-O/SiC(g) remained nearly constant at and below 1273 K, and it decreased at 1573 K. The tensile fracture load of the minicomposite is increased remarkably by the addition of a borosilicate glass powder in the matrix, but the increase was larger at and below 1273 K than at 1573 K. This increase of the tensile fracture load was attributed to more effective load transfer at the fiber/matrix interface for the Si-Ti-C-O/SiC(g) than for the Si-Ti-C-O/SiC. Degradation of the increase at 1573 K is due to the interface degradation decreasing interfacial load transfer capacity.

Keywords: Borosilicate glass powder; Fibres; Mechanical properties; PIP process; Si-Ti-C-O/SiC minicomposite

1. Introduction

Continuous ceramic fiber-reinforced ceramic matrix composites have become an important class of materials for high temperature structural applications.[1–8] Among them, Tyranno® Si-Ti-C-O fiber-reinforced SiC matrix composite fabricated by the polymer infiltration pyrolysis (PIP) process has particularly been studied in recent years because of its excellent potential and relatively simple preparation.[4–8] A major improvement in the mechanical performances of the composites has been achieved by controlling interface properties and fiber properties.[1–4,9,10] Our previous experimental evidence clearly demonstrated the possibility of an interface control procedure for a similar kind of improvement of PIP processed composites.[9–11]

The mechanical properties of PIP-processed SiC base matrix, however, are usually poor and need further improvement.[9–14] For example, the matrix usually contains several pores and it is difficult to avoid their formation because the final ceraming process involves a large shrinkage of the polymer matrix precursor. The existence of pores causes of matrix cracking and rapid oxidation of the composites exposed to high temperature in air.[9–14] Although the multiple PIP processes reduce pore contents, it is difficult to fill completely these pores because of the existence of closely packed pores which formed in initial cycles.[10–14] The addition of SiC and Al_2O_3 particles is another useful procedure to reduce pore content of the matrix.[10–14] This addition helps to reduce shrinkage of the matrix during the ceraming process and thereby improves mechanical properties of the matrix. The problem with the addition of ceramic particles to the matrix is that there is direct contact between the particles and fiber; this reduces interface bonding between the particle and the matrix also acts as a trigger for early stage matrix cracking.

* Corresponding author. Tel.: +81-3-5452-6327; fax: +81-3-5452-6329.
E-mail address: guo@iis.u-tokyo.ac.jp (Y. Kagawa).

0955-2219/$ - see front matter © 2003 Elsevier Ltd. All rights reserved.
doi:10.1016/j.jeurceramsoc.2003.10.044

Thus, a procedure for improvement of the matrix in PIP-processed composites is still an important problem needing resolution. This paper demonstrates the effect of the addition of a glass powder in the matrix on mechanical properties of the composite. To clearly understand the effect of the addition, unidirectionally aligned continuous Si-Ti-C-O fiber-reinforced SiC (Si-Ti-C-O/SiC) and Si-Ti-C-O fiber-reinforced glass powder-dispersed SiC (Si-Ti-C-O/SiC(g)) matrix minicomposites were used.

2. Experimental

2.1. Minicomposite materials

The materials used in the present study were unidirectional continuous Si-Ti-C-O fiber-reinforced SiC and borosilicate glass powder-dispersed SiC matrix minicomposites. Both types were fabricated by the PIP process. Si-Ti-C-O fiber with modified surface chemistry (Tyranno®, TM-S6, Ube Industries Co., Ltd., Ube Yamaguchi, Japan) was used for reinforcement. This fiber had a thin $Si_{45}O_{35}C_{15}Ti_5$ (at.%) surface layer ($\leqslant$10 nm) and a $C_{75}Si_{15}O_8Ti_2$ (at.%) inner layer (10–50 nm) with complicated gradient structure between both the thin layers: the chemical composition near the surface is reported in Ref. 6. This fiber surface treatment is necessary for supplying a weak interface layer between the fiber and the matrix. Its effect is similar to that of carbon and/or BN coatings on Nicalon^{TM} fiber surface. It is found that this surface treatment is effective for improving mechanical properties of Si-Ti-C-O/SiC minicomposites.[9]

Polytitanocarbosilane (Ube Industries Co., Ltd.,) with an average molecular weight of 1300–1400 was dissolved in a xylene solution (content was ≈50 wt.%), and a borosilicate glass powder (content was ≈10 wt.%, Corning Code 7740, Corning, NY, USA) was then added into the solution to form a glass powder-dispersed SiC matrix precursor. The glass powder granules had an average size of 7 μm and the chemical composition was 81 wt.% SiO_2, 13 wt.% B_2O_3, 4 wt.% Na_2O and 2 wt.% Al_2O_3.[15,16] The fiber bundle that contained 800 fibers was continuously infiltrated with the polymer precursor and dried in air at 333 K for 16 h; it was then cut and heated in a high purity N_2 gas flow up to 1473 K at a rate of 100 °C/h and held at that temperature for 15 min. The minicomposite was then cooled to room temperature. This PIP process was repeated twice and the resulting fiber volume fraction of the minicomposite was ≈0.4 (The definition of fiber volume fraction is given in Ref. 9). Moreover, in order to compare the effect of the addition of the borosilicate glass powder on the tensile mechanical behavior of the minicomposite, the same minicomposite without additional glass powder was fabricated by the same process. The fiber volume fraction and the pores of the minicomposite were nearly the same as for the Si-Ti-C-O/SiC(g). The microstructure of the minicomposite was similar to that depicted in a previous report.[9]

2.2. Tensile test

The minicomposites were cut into tensile test specimens with a length of 150 mm. Stainless steel plates ≈1 mm thick and ≈40 mm long were affixed to the gripped area of the specimen to reduce damage caused by the gripping. Water cooling was applied to maintain the load transfer at the gripped portion. Special care was taken to achieve perfect alignment of the minicomposites. Quasi-static monotonic tensile tests were carried out using a servo-hydraulic MTS 808 testing system (MTS System Co., MI, USA) at 298 (room temperature), 1273 and 1573 K. Before tensile loading at 1273 and 1573 K, the specimen was heated to the test temperatures at a rate of 50 °C/min, and was held there for 10 min to achieve uniform temperature distribution at the gauge section (≈60 mm). All the tests at high temperature were done in an argon atmosphere with a constant crosshead displacement rate of 0.1 mm/min. To eliminate the effect of gauge length on the tensile strength of the minicomposite, the gauge length at room temperature was set to 60 mm. Only five specimens were used for each minicomposite due to the limited amount of specimens.

After tensile failure of the minicomposite being tested, the fracture surfaces and other surfaces of both minicomposites were observed by scanning electron microscope (SEM).

3. Results

3.1. Structural characterizations

Fig. 1 shows the X-ray diffraction pattern obtained from the Si-Ti-C-O/SiC and Si-Ti-C-O/SiC(g). The peaks from β-SiC and TiC are detected in both minicomposites. The crystallized α-cristobalite is observed in the Si-Ti-C-O/SiC(g), indicating that part of the added borosilicate glass has crystallized during the fabrication process of the minicomposite. The microstructure of Si-Ti-C-O/SiC(g) is similar to that of Si-Ti-C-O/SiC reported elsewhere[9] (Fig. 2); the residual pores existed with a pore volume fraction of ≈0.06 [Fig. 2(a)]. However, detailed observations revealed that a thin glass-rich layer 0.6–1.0 μm thick was formed on the fiber surface [Fig. 2(b)], and many smaller pores were present in this layer.

Fig. 3 shows the SEM photograph of the polished longitudinal cross-section of the as-fabricated Si-Ti-C-O/SiC(g). Many transverse matrix cracks can be seen

along the fiber axial direction; however, the cracked matrix is still bonded to the fiber without noticeable interface debonding. Although all matrix cracks are formed transversely, the distance between the adjacent crack spacing depends on the location, a crack distance of ≈20 to 60 μm at the zone adjacent to the surface, and a crack distance of ≈10 to 20 μm at the middle zone. In addition, a few smaller matrix fragments are superimposed on the larger matrix fragments.

3.2. Tensile mechanical behavior

3.2.1. Tensile properties

Fig. 4 shows typical load–displacement curves of the Si-Ti-C-O/SiC and Si-Ti-C-O/SiC(g) with test temperature. For Si-Ti-C-O/SiC [Fig. 4(a)], the curves show a nearly linear deformation behavior up to ultimate fracture except in the initial regime of curves due to effect of loading, independent of test temperatures, and the load at fracture of the minicomposite decreases with increasing the test temperature. Differing from Si-Ti-C-O/SiC, the curves of the Si-Ti-C-O/SiC(g) exhibit a linear part near the origin and a large nonlinear behavior from there to the fracture up to 1273 K [Fig. 4(b)]. Although the curve at 1573 K also shows a similar behavior, the nonlinear regime at 1573 K is significantly smaller than that at 298 and 1273 K. Transition of the tensile load–displacement curves from linear to nonlinear behavior tends to initiate at a lower load with increase in test temperature. The transition occurs at load levels around 95 N at 298 and 1273 K, and 85 N at 1573 K, respectively.

Fig. 5 shows plots of tensile fracture load versus test temperature for the Si-Ti-C-O/SiC and Si-Ti-C-O/SiC(g). The addition of a borosilicate glass powder to the matrix substantially increased tensile fracture load of the minicomposite. This increase is significantly larger at and below 1273 K than at 1573 K. The tensile fracture load of the Si-Ti-C-O/SiC(g) is greater by a factor of ~2 to 2.5 than that of the Si-Ti-C-O/SiC, dependent on the tested temperatures. On the other hand, the tensile fracture load of both minicomposites decreases with tested temperature. The decrease in tensile fracture load of the minicomposite tested at 1273 K is ~20 N from that of 298 K and is independent of matrix materials. The decrease in tensile fracture load from 1273 to 1573 K, however, depends on matrix materials: ~80 N for the Si-Ti-C-O/SiC(g) and ~15 N for the Si-Ti-C-O/SiC.

3.2.2. SEM analysis

SEM observations of the failed Si-Ti-C-O/SiC specimens show that the majority of cracked matrix fragments fell off from the individual fibers and even the remaining small matrix fragments are also separated from the fibers [Fig. 6(a)]. Additionally, it is found that the surfaces of the fibers on fracture surface are smooth and without any trace of damage [Fig. 6(b)], in the

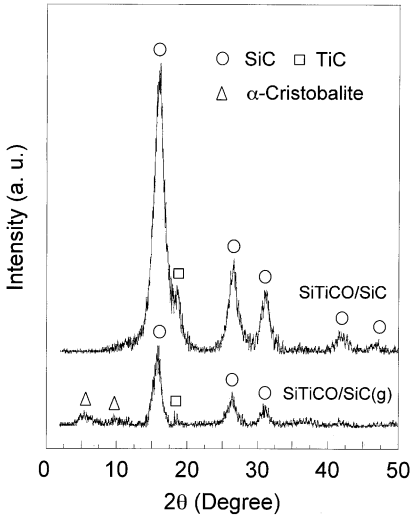

Fig. 1. X-ray diffraction pattern of Si-Ti-C-O/SiC and Si-Ti-C-O/SiC(g), showing existence of a crystallized α-cristobalite in the matrix of Si-Ti-C-O/SiC(g).

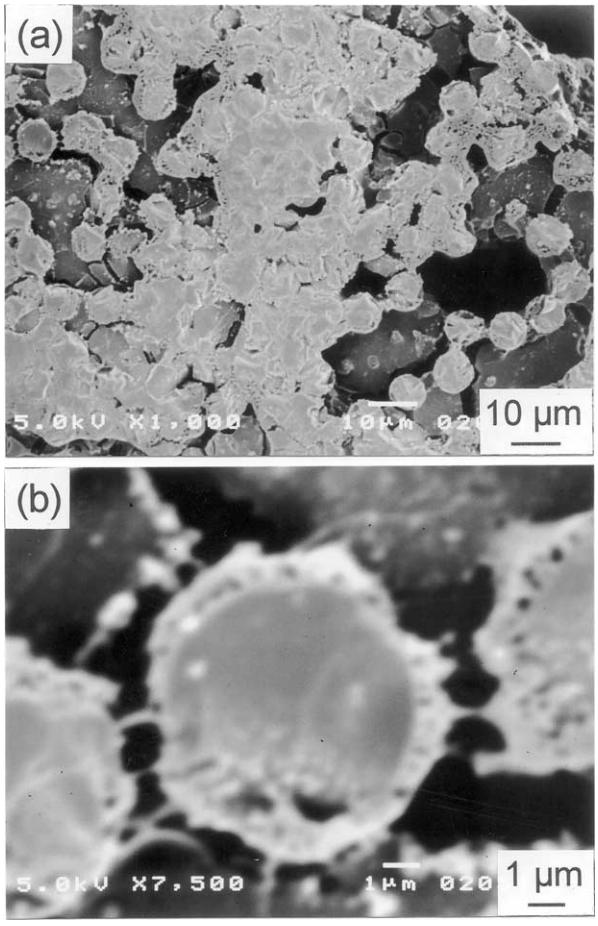

Fig. 2. SEM photographs of the transverse cross-section of Si-Ti-C-O/SiC(g), showing pores (a) and a thin glassy layer on the fiber surface (b).

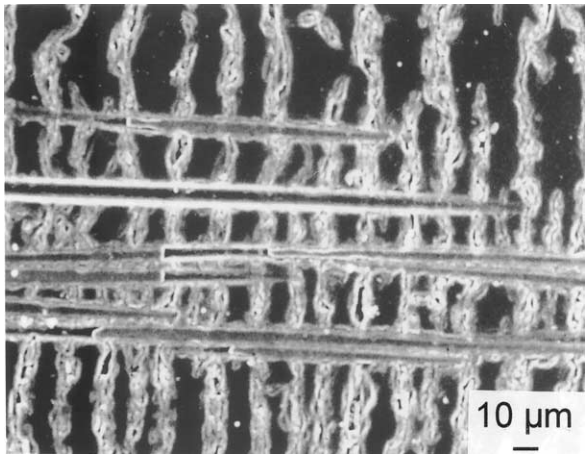

Fig. 3. SEM photograph of the longitudinal cross-section of Si-Ti-C-O/SiC(g), showing multiple matrix cracking behavior along fiber axial direction.

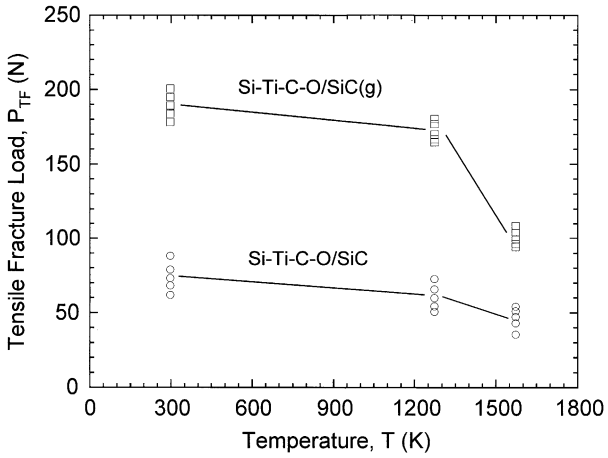

Fig. 5. Tensile fracture load versus test temperature for Si-Ti-C-O/SiC and Si-Ti-C-O/SiC(g).

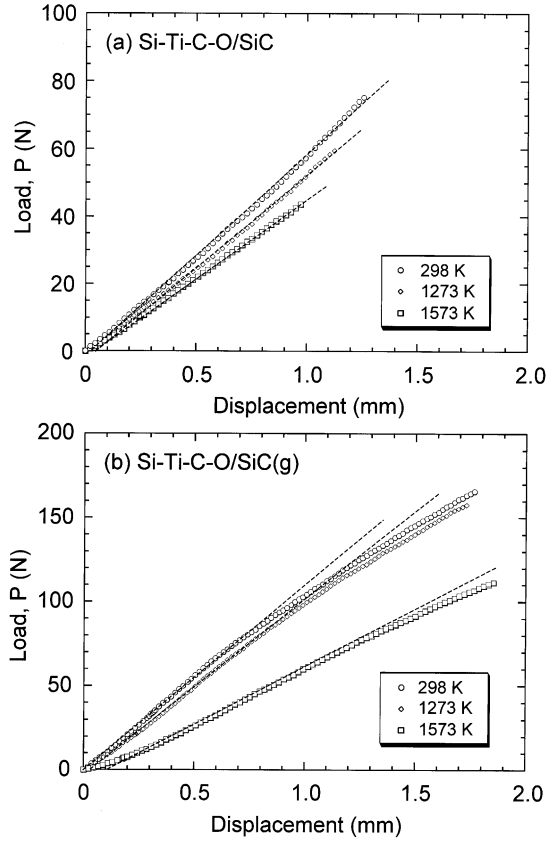

Fig. 4. Typical load–displacement curves of (a) Si-Ti-C-O/SiC and (b) Si-Ti-C-O/SiC(g) with the test temperature.

absence of interface sliding. This matrix fracture behavior occurs independent of the test temperature. In contrast, the surface appearances of the Si-Ti-C-O/SiC(g) after a tensile test are different from Si-Ti-C-O/SiC (Fig. 7). Many uniformly dispersed matrix cracks are observed on the specimens tested at all temperatures. The matrix crack spacing is ≈10 to 20 μm independent of the temperature and this spacing falls in the range of the matrix crack spacing observed in the as-fabricated minicomposite (Fig. 3). Additionally, at 298 K the matrix fragments with a sharp edge and a completely interface debonding behavior are observed [Fig. 7(a)]; while at and above 1273 K the matrix fragments with a dull edge and a bonded interface are exhibited [Fig. 7(b)]. A glassy surface and bridging interface debonding between the fibers and matrix fragments, which is seen on the surface of the specimens tested at and above 1273 K [Fig. 7(b)], is an evidence of the softening of the sealant.

The fracture surfaces of the Si-Ti-C-O/SiC(g) exhibit a typical fibrous appearance by SEM independent of test temperature [Fig. 8(a)]. Surface of the pullout fibers are damaged and some of the matrix fragments are seen on the fiber surface, meaning the presence of interface sliding after interface debonding. Magnification observations indicated that the interface debonding/sliding occurred between the fiber and thin glassy layer [Fig. 8(b)]. The average fiber pullout length, $L_p(g)$, at 298 K is ≈260 μm, and this length decreases with the increase in temperature; the lengths at 1273 and 1473 K are ≈250 and ≈200 μm, respectively.

4. Discussion

4.1. Matrix cracking

Matrix cracking is dependent on the properties of the fibers, the matrix, the fiber architecture, and interphases and interface between the fibers and the matrix. It is found that the tensile mechanical behavior of Si-Ti-C-O/SiC(g) differs significantly from that of Si-Ti-C-O/SiC due to addition of glass powder to matrix. In the Si-Ti-C-O/SiC, the matrix cracking could not be determined from tensile load-displacement curves due to nearly completely linear deformation response up to fracture

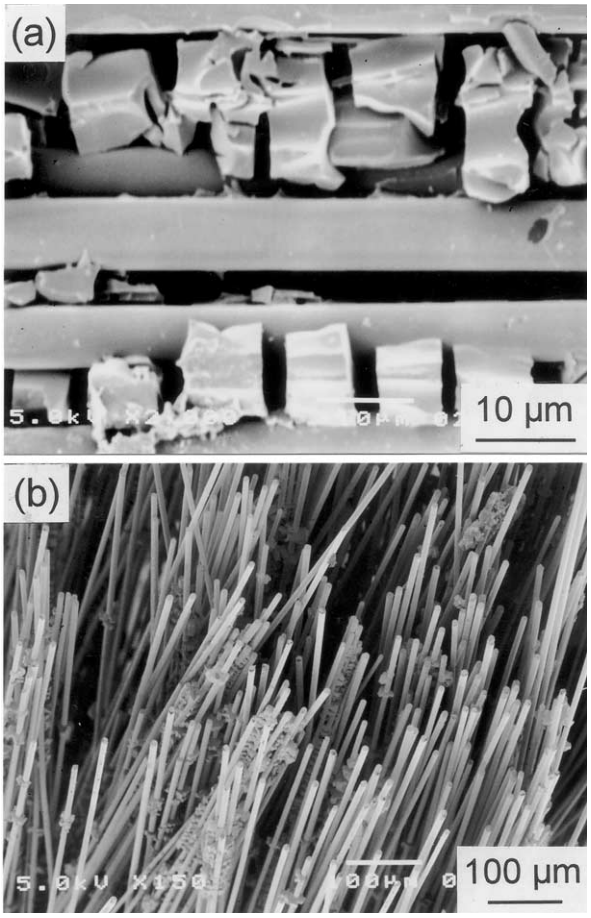

Fig. 6. SEM micrographs of (a) surface appearances and (b) fracture surfaces of post-tested Si-Ti-C-O/SiC ($T = 298$ K).

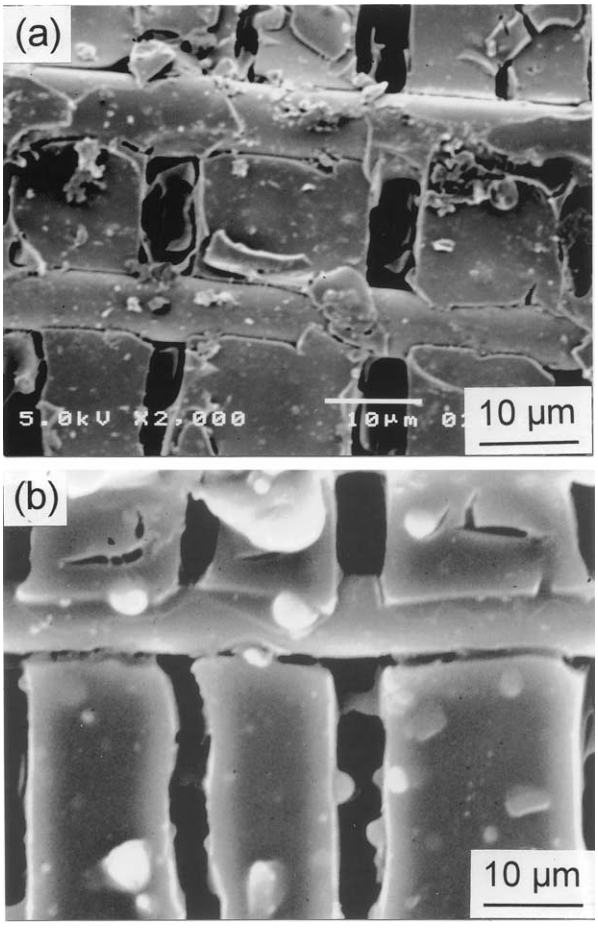

Fig. 7. Typical surface appearances of Si-Ti-C-O/SiC(g) tested at (a) 298 K and (b) 1273 K.

[Fig. 4(a)]. This linear response may be attributed to one of the following two possible fracture cases: (i) a brittle fracture similar to monolithic ceramic due to matrix and interface comparatively strong; and (ii) a tensile fracture response similar to a dry fiber bundle due to very weak matrix and interface bonding.[17] In the present study, the observed very smooth surfaces of the fibers and without any trace of damage on fracture surface of Si-Ti-C-O/SiC [Fig. 6(a)] suggests that the cracked matrix fragments fell off and/or separated from the fibers once the interface debonding occurred no interface sliding, indicating a very weak matrix and the interface bonding between the fiber and the matrix. Thus, it is believed that the linear behavior of Si-Ti-C-O/SiC probably belongs to the above-mentioned latter case. This suggests that the cracked matrix fragments, which formed during ceraming process due to a large shrinkage of a polymer matrix precursor, fell off and/or separated from the fibers once the sample was loaded. Similar behavior was previously reported by Mamiya et al.,[9] who have studied effect of fiber surface modification on tensile fracture behavior of PIP-processed Si-Ti-C-O fiber-reinforced SiC matrix minicomposites.

On the contrary, load–displacement curves with a pronounced nonlinear domain of deformation are observed for the Si-Ti-C-O/SiC(g) [Fig. 4(b)]. The nonlinear behavior is believed in resulting from matrix cracking during tension. The load, at which the transition of the tensile load–displacement curves from linear to nonlinear behavior occurs, is defined as first matrix cracking load. The load remains nearly constant up to 1273 K, and then it decreases as temperature increases from 1273 to 1573 K. This temperature dependence of the matrix cracking force reflects that the softening of the matrix is competing with the interface degradation at high temperatures. The major source of matrix cracking results from originally existing matrix flaws (Fig. 3) due to the matrix crack spacing is nearly consistent with that observed in the as-fabricated minicomposite (Figs. 3 and 7), independent on test temperature. This suggests that the matrix flaws formed during ceraming process still act as a trigger for early stage matrix cracking at room and elevated temperatures. However, the morphology of the cracked matrix fragments and the fiber/matrix interface differed with tested temperatures: (i) at 298 K the matrix fragments

Table 1
Tensile properties of the fibers in Si-Ti-C-O/SiC and Si-Ti-C-O/SiC(g)

Test temperature T (K)	Si-Ti-C-O/SiC			Si-Ti-C-O/SiC(g)		
	σ_b (MPa)	σ_f (MPa)	L_g (mm)	σ_b (g) (MPa)	σ_f (g) (MPa)	L_g (g) (μm)
298	965	1567	60	2538	4121	1044
1273	810	1333	60	2263	3725	984
1573	623	902	60	1205	1745	792

Table 2
Predicted and measured tensile fracture load and tensile strength of Si-Ti-C-O/SiC(g)

Test temperature T (K)	Tensile fracture load, P_{TF} (N)		Tensile fracture strength, σ_{TS} (MPa)	
	Predicted	Measured	Predicted	Measured
298	210	200±12	1112	996±57
1273	190	180±15	997	895±68
1573	100	100±10	509	525±43

with a sharp edge and a completely interface debonding [Fig. 7(a)]; and (ii) at and above 1273 K the matrix fragments with a dull edge and a bonded interface [Fig. 7(b)]. These differences are believed in resulting from softening effect of glass powder added to the matrix at high temperatures and from sealing debonding/sliding interface by less viscous glass phase at high temperatures.

4.2. Tensile fracture load

On the basis of the experimental measurements and observations, assuming that the matrix of the Si-Ti-C-O/SiC completely falls and/or separates from the fibers before a maximum load, the tensile behavior of the minicomposite is considered to be the same as found in a tensile test of a dry fiber bundle with a gauge length of $L_g = 60$ mm (gauge length of specimen). Thus, the tensile strength of the dry fiber bundle, σ_b, in the Si-Ti-C-O/SiC is regarded to be the same as the applied load at fracture divided by the total cross-sectional area of the fibers. Under this assumption, the tensile strength of the fiber, σ_f, with a gauge length of $L_g = 60$ mm is given by[18,19]

$$\sigma_f = \Gamma\left(1 + \frac{1}{m}\right)(me)^{1/m}\sigma_b \quad (1)$$

where Γ is the gamma function, e is the base of natural logarithms, m is Weibull modulus of the fiber and the value of the same minicomposite was reported to be $m = 4.19$ at 298 K, $m = 4.00$ at 1273 K and $m = 6.56$ at 1573 K.[20]

On the other hand, the matrix separation is avoided in the Si-Ti-C-O/SiC(g) because the added glass powder enhances the matrix and interface adhesion (Fig. 7), and thus the effective gauge length, $L_g(g)$, of the fiber in the Si-Ti-C-O/SiC(g) differs from that of the Si-Ti-C-O/SiC. The $L_g(g)$ of the fiber in the Si-Ti-C-O/SiC(g) is given by[21,22]

$$L_g(g) = \frac{4L_P(g)}{\lambda(m)} \quad (2)$$

where $L_p(g)$ is the average fiber pullout length, and $\lambda(m)$ is a nondimensional parameter which is dependent on the fiber fracture statistics and is $\lambda(m) \approx 1$ for $m > 3$.[23] Assuming that the Weibull modulus of the fiber is the same for both minicomposites, and the tensile strength of the fiber, $\sigma_f(g)$, in the Si-Ti-C-O/SiC(g) is given by[19]

$$\sigma_f(g) = \left(\frac{L_g}{L_g(g)}\right)^{1/m}\sigma_f \quad (3)$$

Substituting known values, σ_b, $L_p(g)$, m and L_g, into Eqs. (1)–(3), the tensile strengths of fiber, σ_f and $\sigma_f(g)$, in both minicomposites, tensile strength of the fiber bundle, $\sigma_b(g)$, and effective gauge length, $L_g(g)$, in the Si-Ti-C-O/SiC(g) are obtained, and the obtained values are summarized in Table 1.

When fiber fracture is non-interactive and the global load sharing (GLS) condition is satisfied, the tensile strength, σ_{TS}, of the minicomposite can be computed using the model that was proposed by Curtin[21]

$$\sigma_{TS} = f\sigma_f(g)\left(\frac{2}{m+2}\right)^{1/(m+1)}\left(\frac{m+1}{m+2}\right) \quad (4)$$

where f is the fiber volume fraction. The tensile strength of the Si-Ti-C-O/SiC(g) is predicted using Eq. (4). Table 2 shows a comparison of the tensile strength and tensile fracture load values predicted by Eq. (4) and

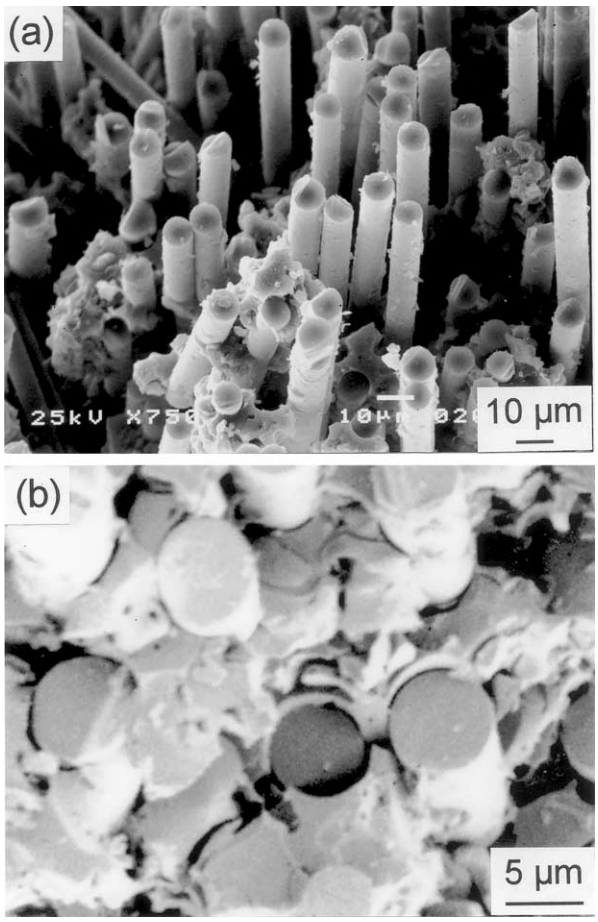

Fig. 8. SEM micrographs of fracture surfaces of Si-Ti-C-O/SiC(g), showing (a) typical fibrous fracture surface and (b) interface debonding between fiber and thin glassy layer ($T = 1573$ K).

measured values for Si-Ti-C-O/SiC(g). Note that the predicted tensile fracture loads are regarded to be the same as the tensile strength values obtained by Eq. (4) multiplied by the total cross-sectional area of the minicomposite. The calculated values of the tensile strength and tensile fracture load of the Si-Ti-C-O/SiC(g) fall within the limits of the experimental values. This indicates that the added glassy powder acts to eliminate the cracked matrix from falling off the fibers, and thus allows a short effective gauge length of the fiber in the minicomposite.

The temperature dependence of the tensile fracture load of the Si-Ti-C-O/SiC is explained by degradation of the fiber strength with increase in test temperature. Although the decrease in the tensile fracture load with temperature is the same for both minicomposites up to 1273 K, at 1573 K this decrease is significantly larger for the Si-Ti-C-O/SiC(g) than for the Si-Ti-C-O/SiC. This indicates that the added glass powder in the matrix of the Si-Ti-C-O/SiC(g) effectively alters the mechanical properties of the minicomposite and this effect continues up to 1273 K. The larger decrease in the tensile fracture load at 1573 K for Si-Ti-C-O/SiC(g) should be

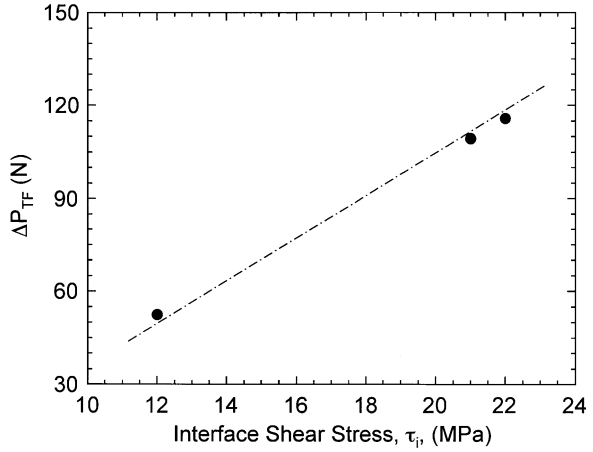

Fig. 9. Reduction in tensile fracture loads of both the minicomposites, ΔP_{TF}, versus interface shear stress, τ_i.

considered the effect of interface degradation at this temperature, except for the degradation of fiber. The interface shear stress, τ_i, of the minicomposite can be represented in terms of the effective gauge length of a fiber as[21]

$$\tau_i(g) = \frac{R_f \sigma_f(g)}{L_g(g)} \tag{5}$$

where R_f (≈5.5 μm) is the radius of the fiber. Substituting known values into Eq. (5), the interface shear stress is obtained and $\tau_i = 22$ MPa at 298K, $\tau_i = 21$ MPa at 1273 K and $\tau_i = 12$ MPa at 1573 K. The interface shear stress decreases with increase in test temperature, and especially significantly at 1573 K. The decrease in the interface shear stress due to increase of temperature is well documented in the literature. Losses in interface shear stress of more than 40 and 70% have been reported for BN-coated Hi-Nicalon™ SiC fiber-reinforced SiC matrix composite tested at 1400 and 1600 K,[24] respectively. Celemin et al.[25] showed that the interfacial shear stress of BN/SiC-coated Nicalon™ SiC fiber-reinforced Al_2O_3 matrix composite reduced by ~30% as this composite was tested at 1473 K. This loss is attributable to relaxation of the interfacial radial residual compressive stresses caused by the thermal expansion mismatch between the matrix and the fiber at high temperature,[24,25] because the coefficient of the thermal expansion (CTE) of the fiber is highly anisotropic and is lower than that of the matrix in radial direction. In particular the residual compressive stresses decreased substantially as the test temperature was above the processed temperature. Similar changes, although not well known due to a lack of CTE data of the Si-Ti-C-O fiber, are expected for the PIP-processed Si-Ti-C-O/SiC(g) minicomposite investigated in this study. Fig. 9 shows the change in reduction in the tensile fracture loads, ΔP_{TS}, of both minicomposites with the interface shear stress, τ_i. It is clear that this reduction is well

correlated with the decreases in the interface shear load transfer potential. Consequently, the large reduction in the tensile fracture load of the Si-Ti-C-O/SiC(g) at 1573 K from that at 1273 K is attributed to poor potential of load transfer at the interface due to interface degradation.

5. Conclusions

The effect of the addition of borosilicate glass powder to the matrix on the tensile strength of PIP-processed Si-Ti-C-O fiber-reinforced SiC matrix minicomposite [Si-Ti-C-O/SiC(g)] was studied. Temperature dependence of the tensile matrix cracking load and tensile fracture load of the minicomposite was obtained and the results are discussed.

A glassy phase was found to be formed at the interface and multiple transverse matrix cracks were observed in the as-fabricated Si-Ti-C-O/SiC(g) minicomposite. The matrix cracking load remained nearly constant at and below 1273 K, while the load decreased at 1573 K. The tensile fracture load of the Si-Ti-C-O/SiC was significantly increased by the addition of the borosilicate glass powder to the matrix, and the increase was significantly larger at and below 1273 K than at 1573 K. The tensile fracture load of the Si-Ti-C-O/SiC(g) increased about 2.5-fold at and below 1273 K and about two-fold at 1573 K over that of the glass powder-free matrix. The increase is attributed to the prevention of the cracked matrix from falling off the fibers and to the strong interfacial adhesion between the fiber and the matrix; these factors cause a decrease in the effective gauge length. The increase degraded at 1573 K because of the ineffective load transfer at the interface caused by interface degradation.

Acknowledgements

The authors would like to thank Drs. M. Fujikura and R. Tanaka, Japan Ultra-High Temperature Materials Research Center Co., Ltd. (JUTEM), for their help in the tensile tests, and Mr. M. Sato and Dr. T. Yamamura, Ube Industries Ltd., for supplying minicomposite materials. This work was supported, in part, by the New Energy and Industrial Technology Development Organization (NEDO), Japan.

References

1. Lee, S. S., Zawada, L. P., Staehler, J. M. and Folsom, C. A., Mechanical behavior and high-temperature performance of a woven Nicalon/Si-N-C ceramic–matrix composite. *J. Am. Ceram. Soc.*, 1998, **81**(7), 1797–1811.
2. Heredia, F. E., Evans, A. G. and Andersson, C. A., Tensile and shear properties of continuous fiber-reinforced SiC™/Al_2O_3 composites processed by melt oxidation. *J. Am. Ceram. Soc.*, 1995, **78**(10), 2790–2800.
3. Sun, E. Y., Nutt, S. R. and Brennan, J. J., High-temperature tensile behavior of a boron nitride-coated silicon carbide-fiber glass–ceramic composite. *J. Am. Ceram. Soc.*, 1996, **79**(6), 1521–1529.
4. Mamiya, T., Kagawa, Y., Shioji, Y., Sato, M. and Yamamura, T., Mechanical properties of coating-free Si-Ti-C-O fiber-reinforced SiC matrix composites. *Key Eng. Mater.*, 1999, **164–165**, 133–136.
5. Kumagawa, K., Yamaoka, H., Shibuya, M. and Yamamura, T., Thermal stability and chemical corrosion resistance of newly developed continuous Si-Zr-C-O tyranno fiber. *Ceram. Eng. Sci. Proc.*, 1997, **18**(3), 113–118.
6. Yamamura, T., Masaki, S., Ishikawa, T., Sato, M., Shibuya, M. and Kumagawa, K., Improvemennt of Si-Ti(Zr)-C-O fiber and a precursor polymer for high temperature CMC. *Ceram. Eng. Sci. Proc.*, 1996, **17**(4), 184–191.
7. Zawada, L. P. and Ishikawa, T., Mechanical behavior of Si-Ti-C-O fiber-bonded ceramic material. *Key Eng. Mater.*, 1999, **164–165**, 245–248.
8. Narisawa, M., Sogame, K., Okamura, K., Sato, M. and Yamamura, T., Tensile creep properties of Si-M-C-O(M = Ti or Zr) fibers in air derived from polymer precursors. *Key Eng. Mater.*, 1999, **164–165**, 303–308.
9. Mamiya, T., Kagawa, Y., Shioji, Y., Sato, M. and Yamamura, T., Tensile fracture behavior and strength of surface-modified Si-Ti-C-O fiber SiC matrix minicomposites fabricated by PIP process. *J. Am. Ceram. Soc.*, 2000, **83**(2), 433–435.
10. Takeda, M., Kagawa, Y., Mitsuno, S., Imai, Y. and Ichikawa, H., Strength of a Hi-Nicalon™/silicon-carbide-matrix composite fabricated by the multiple polymer infiltration-pyrolysis process. *J. Am. Ceram. Soc.*, 1999, **82**(6), 1579–1581.
11. Guo, S. Q. and Kagawa, Y., Temperature dependence of in situ constituent properties of polymer-infiltration-pyrolysis-processed Nicalon™ SiC fiber-reinforced SiC matrix composite. *J. Mater. Res.*, 2000, **15**(4), 951–960.
12. Shin, D. W. and Tanaka, T., Low temperature processing of ceramic woven fabric/ceramic matrix composites. *J. Am. Ceram. Soc.*, 1994, **77**(1), 97–104.
13. Kagawa, Y. and Goto, K., Notch sensitivity of two-dimensional woven fabric SiC–SiC composite fabricated by polymer conversion process. *J. Mater. Sci. Let.*, 1997, **16**, 850–854.
14. Kakisawa, H., Kagawa, Y., Takeda, M., Imai, Y. and Ichikawa, H., Effect of PIP cycles on fracture behavior in unidirectional SiC fiber-reinforced SiC matrix composite. *Adv. Compos. Lett.*, 1999, **8**(3), 1587–1589.
15. Jean, J. H. and Gupta, T. K., Alumina as a devitrification inhibitor during sintering of borosilicate glass powders. *J. Am. Ceram. Soc.*, 1993, **76**(8), 2012–2016.
16. Verma, A. R. B., Murthy, V. S. R. and Murty, G. S., Microstructure and compressive strength of SiC-platelet-reinforced borosilicate composites. *J. Am. Ceram. Soc.*, 1995, **78**(10), 2732–2736.
17. Curtin, W. A., Ahn, B. K. and Takeda, N., Modeling brittle and tough stress–strain behavior in unidirectional ceramic matrix composites. *Acta Mater.*, 1998, **46**(10), 3409–3420.
18. Coleman, B. D., On the strength of classical fibers and fiber bundles. *J. Mech. Phys. Solids*, 1958, **7**, 60–70.
19. Van der Zwaag, S., The concept of filament strength and the Weibull modulus. *J. Testing and Evaluation*, 1989, **17**(5), 292–298.
20. Davies, I. J., Ishikawa, T., Suzuki, N., Shibuya, M., Hirokawa, T. and Gotoh, J., Tensile and in situ fiber properties of 3D SiC/SiC-based composite tested at elevated temperature in vacuum and air with and without an oxidation protection system. *Ceram. Eng. Sci. Proc.*, 1998, **19**(3), 275–282.

21. Curtin, W. A., Theory of mechanical properties of ceramic–matrix composites. *J. Am. Ceram. Soc.*, 1991, **74**(11), 2837–2845.
22. Thouless, M. D. and Evans, A. G., Effect of pullout on the mechanical properties of ceramic matrix composites. *Acta Metall.*, 1988, **36**, 517–522.
23. Beyerle, D. S., Spearing, S. M., Zok, F. W. and Evans, A. G., Damage and failure in unidirectional ceramic–matrix composites. *J. Am. Ceram. Soc.*, 1992, **75**(10), 2719–2725.
24. Guo, S. Q. and Kagawa, Y., Temperature dependence of tensile strength for a woven boron-nitride-coated Hi-Nicalon™ SiC fiber-reinforced silicon–carbide–matrix composite. *J. Am. Ceram. Soc.*, 2001, **84**(9), 2079–2085.
25. Celemin, J. A., Pastor, J. Y., Llorca, J. and Elices, M., Mechanical behavior at 20° and 1200 °C of Nicalon-silicon-carbide-fiber-reinforced alumina–matrix composites. *J. Am. Ceram. Soc.*, 1997, **80**(10), 2569–2580.